Oblique pullout of strip anchor embedded in layered sandbed

Authors:

Rakesh Shambharkar, MCE
Visvesvaraya National Institute of Technology
Department of Civil Engineering
dt20civ017@students.vnit.ac.in
Corresponding author

Assist.Prof. **Srinivasan Venkatraman**, PhD. CE
Visvesvaraya National Institute of Technology
Department of Civil Engineering
srinivasanv@civ.vnit.ac.in

Assist.Prof. **Santhoshkumar Gunasekaran**, PhD. CE
Indian Institute of Technology, Bhubaneswar
School of Infrastructure
santhoshg@iitbbs.ac.in

Pareese Pathak, BCE
Visvesvaraya National Institute of Technology
Department of Civil Engineering
pareespathak@gmail.com

Research Paper

Rakesh Shambharkar, Srinivasan Venkatraman, Santhoshkumar Gunasekaran, Pareese Pathak

Oblique pullout of strip anchor embedded in layered sandbed

This study analyzes the vertical and oblique pullout behavior of a strip anchor plate horizontally embedded in homogeneous and two-layered sandy soil layers. The analysis was performed using the limit equilibrium method combined with Kötter's equation. The research results concerning the pullout capacity of the anchor are presented using a dimensionless parameter known as the pullout factor ($K = P_u/\gamma_{avg}b^2$), where P_u is the gross pullout load, γ_{avg} is the weighted average unit weight of two layers of soil, and b is the width of the anchor plate). The findings indicate that the value of the pullout factor increases as the angle of oblique pullout increases for a given embedment depth, and a significant reduction in the pullout capacity is observed at lower embedment depths for a particular friction angle. The study also investigated the impact of various parameters, such as the unit weight of the soil, internal friction, embedment depth, and orientation of the tie rod. A comprehensive parametric analysis was conducted to understand these effects in detail. The outlined approach, based on Kötter's equation, provides a simplified method for anticipating the optimal design and placement of anchors in sandy soils. This study serves as a foundational step toward achieving effective anchor design and installation strategies in sand-based environments.

Key words:

anchors, failure load, Kötter's equation, limit equilibrium, optimization, pullout

Prethodno priopćenje

Rakesh Shambharkar, Srinivasan Venkatraman, Santhoshkumar Gunasekaran, Pareese Pathak

Koso izvlačenje trakastog sidra ugrađenog u uslojenu pješčanu podlogu

Ovo istraživanje analizira ponašanje vertikalnog i kosog izvlačenja trakaste sidrene ploče, horizontalno ugrađene u homogena i uslojena pjeskovita tla. Analiza je provedena metodom granične ravnoteže u kombinaciji s Kötterovom jednadžbom. Rezultati istraživanja koji se odnose na sposobnost izvlačenja sidra prikazani su pomoću bezdimenzijskog parametra poznatog kao faktor izvlačenja ($K = P_u/\gamma_{avg}b^2$), gdje P_u je bruto opterećenje izvlačenja, γ_{avg} je ponderirana prosječna zapreminska težina dvaju slojeva tla, i b je širina sidrene ploče). Rezultati dokazuju da se vrijednost faktora izvlačenja povećava kako se kut kosog izvlačenja povećava za danu dubinu ukopanosti, a značajno smanjenje kapaciteta izvlačenja opaža se na manjim dubinama ukopanosti za određeni kut trenja. Istraživanje se također bavilo utjecajem različitih parametara, kao što su jedinična težina tla, unutarnje trenje, dubina ukopanosti i usmjerenje spojne šipke. Provedena je opsežna parametarska analiza kako bi se razumio svaki učinak. Navedeni pristup, temeljen na Kötterovoj jednadžbi, pruža pojednostavljenu metodu za predviđanje optimalnog oblika i postavljanja sidara u pjeskovitim tlima. Ovo istraživanje služi kao temeljni korak prema postizanju učinkovitog oblika sidra i strategijama za ugradnju u pjeskovitim okruženjima.

Ključne riječi:

sidra, opterećenje do sloma, Kötterova jednadžba, granična ravnoteža, optimizacija, izvlačenje

1. Introduction

Anchors embedded in soil are commonly used to ensure stability in the foundation systems of various structures, such as transmission towers, dry docks, chimneys, buried pipelines, communication towers, ocean platforms, and earth retention structures. Several researchers have studied the vertical pullout capacity of anchors embedded horizontally in homogeneous cohesionless soil using different methodologies, including the limit equilibrium method [1-11], experimental and laboratory model tests [12-18], the finite element method [19, 20], and upper and lower bound limit analysis [21-26]. Among the available methodologies, the limit equilibrium method coupled with Kötter's equation [27] is a widely used approach for determining the pullout of anchors in soil due to its simplicity [3-6, 28-32]. Various methods can be employed to determine the pullout, depending on soil properties [33, 34], anchor and tie-rod positions [18, 26, 32], placement depth [2, 5, 14], anchor width [19], anchor shape [3, 21, 23], and anchor orientation [15].

Liu et al. [14] and Ilamparuthi et al. [17] conducted experiments and observed that the failure envelope of a shallow circular anchor was a truncated cone with a planar failure surface. Similarly, previous researchers such as Mors [7], Down and Chieurzzi [8], Matsuo [9], and Veesaert and Clemence [10] assumed the failure surface to be a truncated cone when determining the pullout capacity of a circular anchor using a theoretical approach. For horizontal strip anchors, Murray and Geddes [13], Kumar and Kouzer [11], Deshmukh et al. [3-6], and Rangari et al. [28-32] considered a planar failure surface originating from the edge of the anchor plate in the limit analysis method.

Previous studies have mostly focused on vertical pullout and homogeneous soil conditions; however, in reality, soil is often heterogeneous, with varying strength profiles at different depths. Additionally, various factors, such as soil properties, loading conditions, embedment ratio, and the shape and orientation of the anchors, may influence the pullout capacity of the anchors. This study investigates the behavior of strip anchors embedded in a layered sand system subjected to oblique pullout loads. Thus, the findings of this study can significantly contribute to the design and installation of anchor systems for structures subjected to oblique loading, such as mooring for offshore renewable energy devices and other floating structures subjected to uplift forces.

The pullout of an anchor is primarily governed by the shear strength properties of the soil [13]. Therefore, the magnitude of the maximum pullout capacity (Pu) is normalized to the soil properties, specifically the unit weight of the soil within the assumed failure zone, and the results are expressed in a nondimensional pullout factor (K) for better understanding and field implementation. To determine the maximum pullout factor (K) of the anchor plate, the ultimate resistance of the soil medium to the pullout load on the anchor plate was computed. This computation involved analyzing the stability of the soil mass above the anchor plate and calculating the factor of safety (FOS) against the potential failure of the soil mass. The safety factor is defined as the ratio of the resisting forces to the driving forces and must be greater than unity for the system to be stable. Furthermore, the effects of various parameters, such as soil properties, embedment ratio, oblique angle of the pullout, unit weight of the soil, and the optimum failure surface of the soil, may also have a significant impact on the analysis. Therefore, a detailed analysis considering these observations must be conducted to address the prevalent issues pertaining to anchor foundation systems.

2. Problem definition

A strip anchor plate of width "b" is embedded in a layered sandy stratum at a depth "H" below the ground level, as illustrated in Figure 1. The thickness of the plate is negligible compared to its width (b), hence the weight of the anchor does not significantly affect the analysis. The soil mass above the plate consists of two different sand layers with thicknesses H_T and H_B corresponding to the top and bottom layers, respectively, as shown in Figure 1. The primary objective is to determine the magnitude of the maximum pullout factor (K) of the anchor plate while it is placed horizontally at an embedment depth of H. The inclination of the tie rod (β) varies from 0° to less than ϕ. The failure surface is typically linear, and the soil medium is assumed to follow the Mohr–Coulomb failure criterion. The study involves determining the magnitude of the maximum pullout factor by considering various parameters such as the layers of soil (ϕ_T and ϕ_B), the embedment ratio ($\lambda = H/b$), the oblique angle of the pullout (β), the unit weight of the soil (γ), and the optimum failure surface of the soil (α).

Figure 1. Plate Anchor embedded in the two-layer sand stratum

The following assumptions were made:
- The anchor plate obeys the plane-strain condition; hence, it is treated as a two-dimensional problem.
- The anchor plate is perfectly smooth.
- The anchor tie rod has no influence on the failure load or on the pattern of failure.
- The soil at failure follows the Mohr-Coulomb failure criterion.
- The failure surface is presumed to be a straight line originating from the edges of the anchor toward the ground surface.
- The soil mass below the anchor is assumed to not offer any resistance to the pullout force.

3. Analysis and formulation

Formulation to conduct a limit equilibrium analysis, a feasible failure surface must be assumed. The analysis was performed by equating the forces within the assumed failure domain. It must be noted that the failure surface is traced from a pivot point, as shown in Figure 2, to facilitate the inclusion of Kötter"s formulation [27]. Thus, the force due to the soil reaction on the failure surface can be obtained using Eqs. (1) and (3).
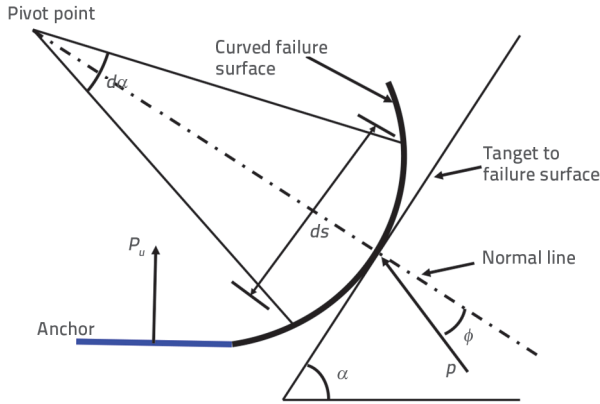
Figure 2. Idealized representation curved failure surface for application to Kötter"s expression

3.1. Distribution of soil reaction on the failure surface

Kötter"s equation for the passive state of equilibrium under plane-strain conditions in sand was used to obtain the distribution of the soil reaction on a curved surface, as shown in Figure 2, and is expressed in the following form:

$$\frac{dp}{ds} + 2p \cdot \tan\phi \frac{d\alpha}{ds} = \gamma \sin(\alpha + \phi) \tag{1}$$

Where, dp is the differential reaction pressure on the failure surface, ds is the differential length of the failure surface, ϕ is the angle of soil internal friction, $d\alpha$ is the incremental change in the angle of the failure plane (α), γ is the unit weight of soil.

Since the failure surface is assumed to be in the form of a straight line originating from the edges of the strip anchor at an angle (α), with respect to the horizontal and meeting the ground surface as shown in Figure 3. Eq. (1) can be reduced to

$$\frac{dp}{ds} = \gamma\sin(\alpha + \phi) \tag{2}$$

Integrating the Eq. (2),

$$p = s\gamma\sin(\alpha + \phi) + C_1 \tag{3}$$

where C_1 is an integration constant obtained from the available boundary conditions. In this study, the sand layer consisted of two layers, assuming that the failure surfaces were a series of straight lines (i.e. DE, EF, GJ, and JA), as shown in Figure 3.a. Hence, the reaction forces R_{RT}, R_{RB}, R_{LB} and R_{LT} on the failure surfaces on both sides of the strip anchor can be obtained using Eq. (3) with appropriate boundary conditions: It is noteworthy that the nomenclature is followed in the analysis in such a way that the first subscripts $_R$ and $_L$ refer to the right and left sides of the centreline of the anchor, respectively. The second subscripts $_T$ and $_B$ refer to the top and bottom sand layers, respectively.

3.1.1. Reaction force along DE

For the failure surface DE, from Eq. (3), D is the initial point of measurement of failure surface DE.

In point D, $s_D = 0 \rightarrow p_D = 0 \rightarrow C_1 = 0$

Hence, Eq. (3) deduces to

$$p_{DE} = s_{DE}\gamma_T\sin(\alpha_{RT} + \phi) \tag{4}$$

The pullout force (Figure 3.a) was resisted by R_{RT} of the resultant soil reaction for the failure surface DE. Integrating Eq. (4) over the surface DE, the reaction R_{RT} on the failure surface can be obtained as
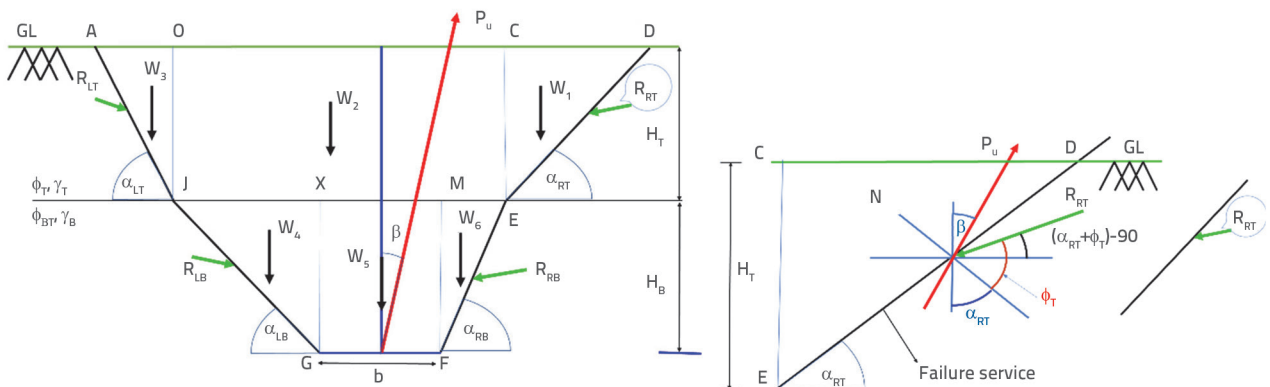
Figure 3. Admissible failure mechanism: a) Geometry; b) Soil reactions

$$R_{RT} = \left[\frac{s_{DE}^2}{2}\gamma_T\sin\left(\alpha_{RT}+\phi_T\right)\right]_0^{DE}$$

$$R_{RT} = \frac{DE^2\gamma_T\sin\left(\alpha_{RT}+\phi_T\right)}{2}$$

(5)

From Figure 3.a, utilizing geometry, it can be expressed as Eq (6),

$$R_{RT} = \frac{\gamma_T H_T^2\sin\left(\alpha_{RT}+\phi_T\right)}{2\left[\sin\left(\alpha_{RT}\right)\right]^2}$$

(6)

3.1.2. Reaction force along EF

For failure surface EF, Eq. (3) can be written as

$$p_{EF} = s_{EF}\gamma_B\sin(\alpha_{RB}+\phi_B)+C_2$$

(7)

At Point
$s = s_{EF} = s_E = 0$ i $p = p_{EF} = p_E = \dfrac{\gamma_T H_T\sin\left(\alpha_{RT}+\phi_T\right)}{\left[\sin\left(\alpha_{RT}\right)\right]}$

and substituting in equation (7), C_2 yields as

$$C_2 = \frac{\gamma_T H_T\sin\left(\alpha_{RT}+\phi_T\right)}{\left[\sin\left(\alpha_{RT}\right)\right]}$$

Similar to the top layer, the reaction force for the bottom layer can be expressed by substituting appropriate boundary conditions as follows:

$$R_{RB} = \frac{\gamma_B\left(H-H_T\right)^2\sin\left(\alpha_{RB}+\phi_B\right)}{2\left[\sin\left(\alpha_{RB}\right)\right]^2} + \frac{\gamma_T H_T\sin\left(\alpha_{RT}+\phi_T\right)\left(H-H_T\right)}{\left(\sin\ \alpha_{RT}\right)\left(\sin\ \alpha_{RB}\right)}$$

(8)

Similarly, the soil reactions R_{LT} and R_{LB} on failure surfaces AJ and JG can be calculated using Eqs. (6) and (8), respectively.

$$R_{LT} = \frac{\gamma_T H_T^2\sin\left(\alpha_{LT}+\phi_T\right)}{2\left[\sin\left(\alpha_{LT}\right)\right]^2}$$

(9)

$$R_{LB} = \frac{\gamma_B\left(H-H_T\right)^2\sin\left(\alpha_{LB}+\phi_B\right)}{2\left[\sin\left(\alpha_{LB}\right)\right]^2} + \frac{\gamma_T H_T\sin\left(\alpha_{LT}+\phi_T\right)\left(H-H_T\right)}{\left(\sin\alpha_{LT}\right)\left(\sin\alpha_{LB}\right)}$$

(10)

3.2. Weight of soil mass (*W*)

The weight of the soil mass (*W*) enclosed by the ADEFGJ failure surface can be obtained by summing the weights of the individual blocks (DCE, CEJO, AOJ, JXG, XMFG, and EMF), as shown in Fig. 3.a.

$$W = \left[\begin{array}{c}\frac{\gamma_T H_T^2}{2\tan\alpha_{RT}} + \frac{\gamma_T H_T\left(H-H_T\right)}{\tan\alpha_{RB}} + \gamma_T H_T b + \frac{\gamma_T H_T\left(H-H_T\right)}{\tan\alpha_{LB}} + \frac{\gamma_T H_T^2}{2\tan\alpha_{LT}}\\[2mm] + \frac{\gamma_B\left(H-H_T\right)^2}{2\tan\alpha_{LB}} + \gamma_B b\left(H-H_T\right) + \frac{\gamma_B\left(H-H_T\right)^2}{2\tan\alpha_{RB}}\end{array}\right]$$

(11)

3.3. Pullout of an anchor

The analysis was carried out within the framework of limit equilibrium; thus, the forces obtained in the previous section were equated to maintain equilibrium in the soil domain ADEFGJ. Consequently, the pullout (P_u) of the anchor associated with the trapped soil domain can be obtained as

$$Pu = [W\cos\beta - R_{RT}\cos(\alpha_{RT}+\beta+\phi_T) - R_{RB}\cos(\alpha_{RB}+\beta+\phi_B)$$
$$- R_{LT}\cos(\alpha_{LT}-\beta+\phi_T) - R_{LB}\cos(\alpha_{LB}-\beta+\phi_B)]$$

(12)

Substituting R_{RT}, R_{RB}, R_{LT}, R_{LB}, and W into Eqs. (6), (8), (9), (10), and (11), respectively, in Eq. (12)

$$P_u = \left\{\begin{array}{c}\left[\begin{array}{c}\frac{\gamma_T H_T^2}{2\tan\alpha_{RT}} + \frac{\gamma_T H_T(H-H_T)}{\tan\alpha_{RB}} + \gamma_T H_T b + \frac{\gamma_T H_T(H-H_T)}{\tan\alpha_{LB}} + \frac{\gamma_T H_T^2}{2\tan\alpha_{LT}}\\ + \frac{\gamma_B(H-H_T)^2}{2\tan\alpha_{LB}} + \gamma_B b(H-H_T) + \frac{\gamma_B(H-H_T)^2}{2\tan\alpha_{RB}}\end{array}\right]\cos\beta\\[3mm] -\left[\frac{\gamma_T H_T^2\sin(\alpha_{RT}+\phi_T)}{2(\sin\alpha_{RT})^2}\right]\cos(\alpha_{RT}+\beta+\phi_T)\\[2mm] -\left[\frac{\gamma_B(H-H_T)^2\sin(\alpha_{RB}+\phi_B)}{2(\sin\alpha_{RB})^2} + \frac{\gamma_T H_T\sin(\alpha_{RT}+\phi_T)\times(H-H_T)}{(\sin\alpha_{RT})(\sin\alpha_{RB})}\right]\cos(\alpha_{RB}+\beta+\phi_B)\\[2mm] -\left[\frac{\gamma_T H_T^2\sin(\alpha_{LT}+\phi_T)}{2(\sin\alpha_{LT})^2}\right]\cos(\alpha_{LT}-\beta+\phi_T)\\[2mm] -\left[\frac{\gamma_B(H-H_T)^2\sin(\alpha_{LB}+\phi_B)}{2(\sin\alpha_{LB})^2} + \frac{\gamma_T H_T\sin(\alpha_{LT}+\phi_T)(H-H_T)}{(\sin\alpha_{LT})(\sin\alpha_{LB})}\right]\cos(\alpha_{LB}-\beta+\phi_B)\end{array}\right\}$$

(13)

The results are presented in the form of a dimensionless parameter, that is, the pullout factor (*K*) of the anchor, to provide a meaningful parametric study, as expressed in Eq. (14),

$$K = \frac{P_u}{\gamma_{avg}b^2}$$

(14)

γ_{avg} = Weighted average of the unit weights of two layered sand which can be calculated from,

$$\gamma_{avg} = \frac{\gamma_T H_T + \gamma_B H_B}{H}$$

4. Results and discussion

4.1. Validation of results

4.1.1. Validation for homogeneous cohesionless soil

To validate the current results, a breakout factor ($q_u = P_u/\gamma bH$) identified from the literature by Rangari et al. [29] was used. Table 1 presents a comparison of the breakout factor values from the current study with those from other studies [1, 5, 11, 18, 29], which employed various methods such as limit equilibrium, upper-bound limit analysis, and experimental observation. Given parameters γ =14.5 kN/m³, b = 1 m, β = 0°, ϕ = 35°, the methods proposed by Deshmukh et al. [5], and Rangari et al. [29], and Kumar and Kouzer [11] showed better conformity with the experimental results of Dickin [18]. However, the results obtained by Meyerhof and Adams [1] overestimated the pullout capacity compared to the

Table 1. Comparison of computed breakout factor ($q_u = P_u/\gamma bH$) from [29] for a strip anchor in a Single-Layer Homogeneous Sandy Medium by considering γ =14.5 kN/m³, b = 1 m, β = 0°, ϕ = 35°

$\lambda = H/b$	Meyerhof and Adams [1] ($\delta = 2\phi/3$)	Deshmukh et al.[5] ($\delta = \phi$)	Rangari et al.[29] ($\delta = 2\phi/3$)	Dickin [18] (Exp. work)	Kumar and Kouzer [11] ($\delta = \phi$)	Present study ($\delta = \phi$)
1	1.89	1.63	1.69	1.52	1.70	1.70
2	2.70	2.26	2.39	1.89	2.40	2.40
3	3.54	2.89	3.08	2.29	3.10	3.10
4	4.16	3.52	3.79	3.01	3.80	3.80
5	4.83	4.15	4.48	3.20	4.50	4.50

Table 2. Comparison of Oblique breakout factor ($P_u/\gamma bH$) for a strip anchor in the Homogeneous sand with ϕ = 31°, for different embedment ratio

β (°)	Das and Seeley [12] (Experimental paper)			Rangari et al.[32] ($\delta = 2\phi/3$)			Present study ($\delta = \phi$)		
	λ = 1	λ = 2	λ = 4.5	λ = 1	λ = 2	λ = 4.5	λ = 1	λ = 2	λ = 4.5
0	1.53	2.08	3.29	1.58	2.17	3.65	1.60	2.20	3.70
10	1.79	2.99	3.91	1.73	2.37	3.97	1.63	2.25	3.82
20	2.44	3.92	4.37	1.96	2.68	4.5	1.72	2.43	4.23
30	2.76	4.49	4.57	2.34	3.21	5.39	1.92	2.85	5.16
40	3.23	4.84	4.86	3.06	4.16	6.97	NA*	NA*	NA*

NA* - As the present study considers obliquity angle (β) ≤ friction angle (ϕ)

experimental results. The current values match exactly with those of Kumar and Kouzer [11], as β = 0°, which bolsters the authenticity of the proposed formulation. The wall friction considered in Kumar and Kouzer [11] and in the current study is rigid ($\delta = \phi$), whereas the method adopted by Rangari et al. [29], which used a different wall friction angle ($\delta = 2\phi/3$), resulted in overestimated outcomes. Table 1 also shows that the results are overestimated when the wall friction angle is considered to be ($\delta = 2\phi/3$).

Table 2 compares the breakout factor ($q_u = P_u/\gamma bH$) in medium-dense sand for the test data from Das and Seeley [12], with b = 0.064 m and γ = 14.71 kN/m³, ϕ = 31° for the various inclinations of oblique load. For lower embedment ratios (λ = 1 & 2), the present study underestimates the experimental results as obliquity increases. However, for higher embedment depths (λ = 4.5), the proposed theory closely follows the experimental results for oblique pullout angles of 10° and 20°, exhibiting percentage errors of 2.30 % and 3.20 %, respectively. Smaller embedment depths may be more affected by local soil variability, suggesting that the assumed linear failure surface may need revision. For greater embedment depths, the influence of local soil variability may be reduced, and the linear failure surface suffices to capture the pullout behavior, leading to similar predicted values.

Rangari et al. [32] and this study used Kötter"s equation to predict the pullout capacity. The small variation observed in Table 2 could be attributed to the contribution of passive resistance from the inner soil wedge, with the wall friction angle considered as ($\delta = 2\phi/3$). Rangari et al. [32] estimated a slightly higher pullout capacity than that obtained in the present study.

4.1.2. Validation for two layers from literature

To validate the accuracy of the present analysis, the pullout factor (K) values obtained from the present study were compared with the upper-bound results of Kumar [21] based on the assumption of a linear collapse mechanism, as shown in Figure 4. It should be noted that the present analysis was conducted within the framework of limit equilibrium. Because no comprehensive studies have been carried out on the uplift capacity of anchors in layered soil using the limit equilibrium approach, validation was carried out using the available upper-bound limit analysis method [21].

It is worth mentioning that the upper-bound method requires a kinematically admissible failure mechanism, followed by an optimization study to obtain the least upper-bound solution. However, limit equilibrium does not require rigorous optimization studies. The results obtained in the present study are very close to those of Kumar [21], indicating that the present

limit equilibrium approach accurately simulates two-layered sand conditions without the rigorous computations required in the upper-bound limit analysis.
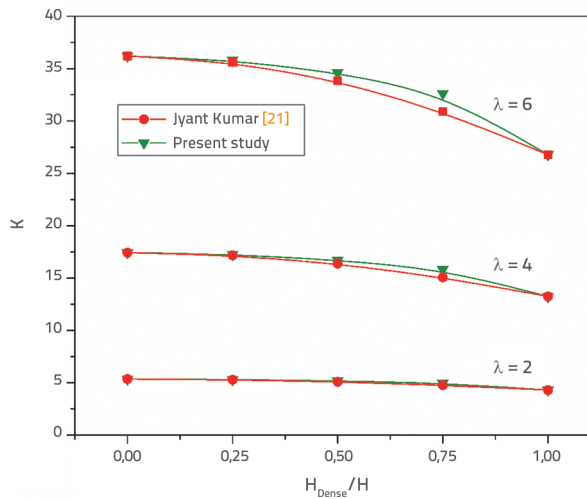
Figure 4. Comparison of the present pullout factor with the upper-bound limit analysis of Jyant Kumar [21] for strip anchor top layer loose and bottom layer dense

4.2. Homogeneous cohesionless soil

This section evaluates the validity of the proposed formulation. Eq. (14) can be used to estimate the pullout factor (K) for a layered sand profile. However, the formulation simplifies to the same analytical expression for calculating K for a strip anchor embedded in homogeneous sand if the top and bottom layers are identical, as shown below:

$$\phi_T = 0, \phi_B = \phi \text{ and } \gamma_T = 0, \gamma_B = \gamma \qquad (15a)$$

$$\phi_T = \phi, \phi_B = 0 \text{ and } \gamma_T = \gamma, \gamma_B = 0 \qquad (15b)$$

As Eq. (13) demonstrates, the pullout (P_u) is sensitive to several parameters. Therefore, an optimization study was conducted on the failure angles for the different ranges of parameters reported in Table 3. The subsequent sections discuss the effects

of the failure surface, soil friction angle, embedment ratio, and orientation of the tie rod on homogeneous cohesionless soil using Eq. (15a) and (15b).

Table 3. Range of the parameters varied in the analyses

Parameters	Range of values
Inclination of pullout load, β^o	0° to $< \phi^o$
Angle of soil friction, ϕ^o	20°, 30°, 40°
Embedment ratio, H/b, λ	2, 4, 6
Ratio of densities, γ_T / γ_B	1.5, 1.25, 1, 0.75, 0.5
H_{dense} / H	0, 0.25, 0.5, 0.75, 1

4.2.1. Failure surfaces

The study reveals that the inclination of the failure surfaces on the right and left sides of an anchor is affected by the orientation of the tie rod (β), which in turn influences the soil reactions on either side of the anchor. The maximum pullout was achieved when the reaction component was reduced to zero, which correlated with the failure surface angle.

Interestingly, the embedment ratio did not affect the angle of inclination of the failure planes under either oblique or vertical pullout, as shown in Table 4 and Figure 5. The same observation was corroborated by the predictions made by [12, 30, 32] for oblique pullout.

4.2.2. Effect of soil friction angle (ϕ)

As observed in Figure 6, the pullout factor (K) consistently increases with an increase in the soil friction angle (ϕ) for different embedment ratios (λ). For instance, when the friction angle is increased from $20°$ to $40°$, the vertical pullout factor at an embedment ratio $\lambda = 4$, increases by 77.4%, as shown in Figure 6.a. A similar increase in the pullout factor is observed in Figure 6.b, where the percentage increase in the oblique pullout factor is about 81 % at $\beta = 10°$ and $\lambda = 4$. It can be reasonably stated that the magnitude of K increases with an increase in ϕ and β as well, for a given embedment ratio λ. Thus, the pullout of the anchors can be significantly improved by optimizing
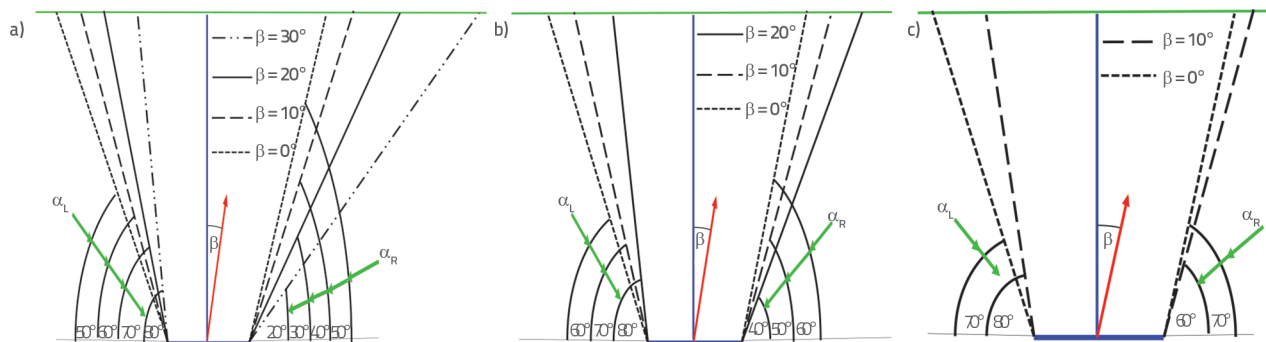
Figure 5. Geometrical representation of failure angle for embedment ratio ($\lambda = 2, 4, \& 6$) for various friction angle: a) $\phi = 40°$; b) $\phi = 30°$; c) $\phi = 20°$

Table 4. Failure angles and Uplift pullout factor for different embedment ratio

Sr. No.	ϕ [°]	$\lambda = 2$				$\lambda = 4$				$\lambda = 6$			
		β [°]	α_R [°]	α_L [°]	K	β [°]	α_R [°]	α_L [°]	K	β [°]	α_R [°]	α_L [°]	K
1	20	0	70	70	3.455	0	70	70	9.822	0	70	70	19.101
2	20	10	60	80	3.454	10	60	80	9.877	10	60	80	19.269
3	30	0	60	60	4.308	0	60	60	13.235	0	60	60	26.78
4	30	10	50	70	4.339	10	50	70	13.417	10	50	70	27.235
5	30	20	40	80	4.45	20	40	80	14.043	20	40	80	28.778
6	40	0	50	50	5.355	0	50	50	17.422	0	50	50	36.199
7	40	10	40	60	5.454	10	40	60	17.877	10	40	60	37.269
8	40	20	30	70	5.818	20	30	70	19.515	20	30	70	41.091
9	40	30	20	80	6.796	30	20	80	23.721	30	20	80	50.773
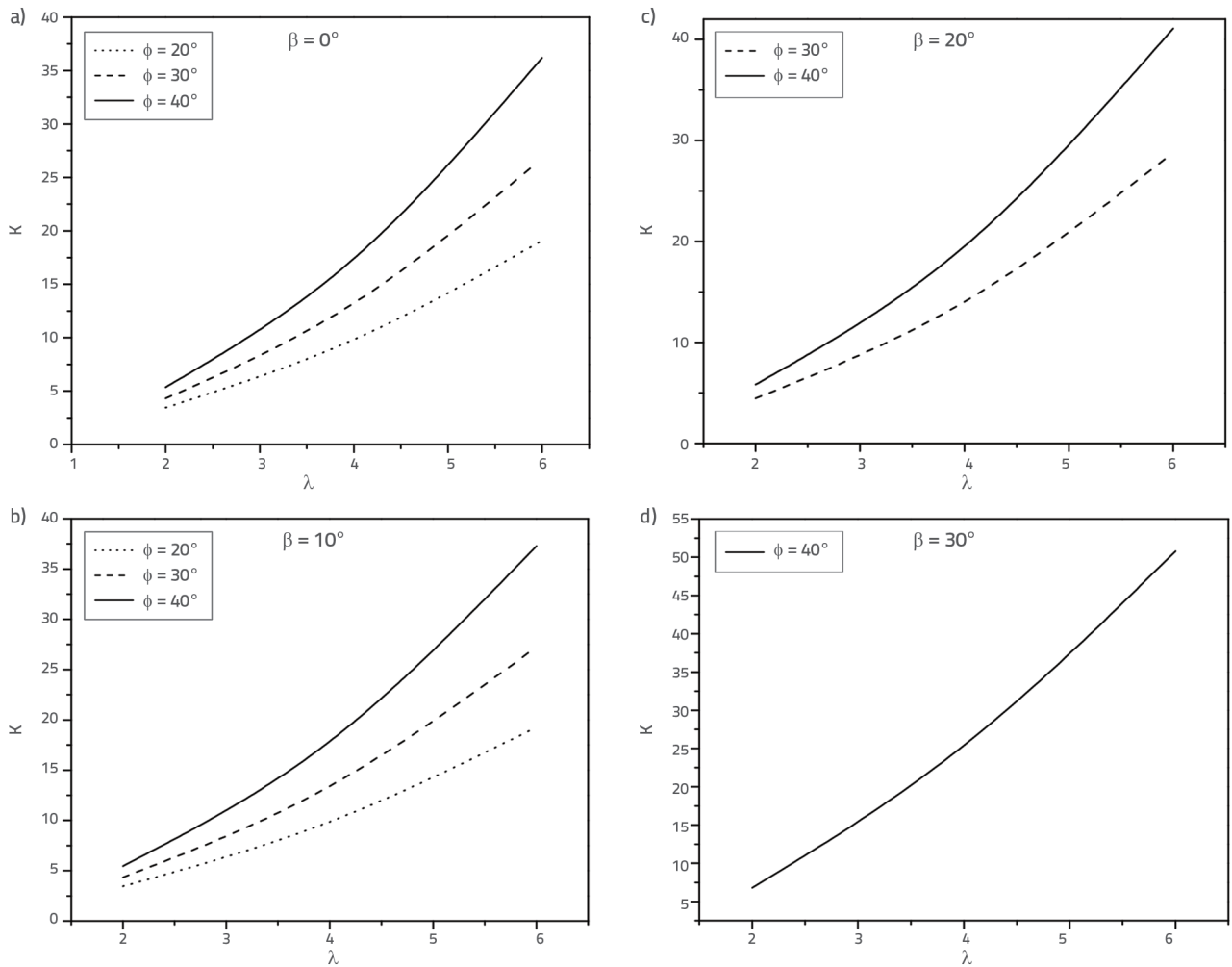
Figure 6. Variation of pullout factor (K) with embedment ratio (λ) for different values of ϕ: a) $\beta = 0°$; b) $\beta = 10°$; c) $\beta = 20°$; d) $\beta = 30°$
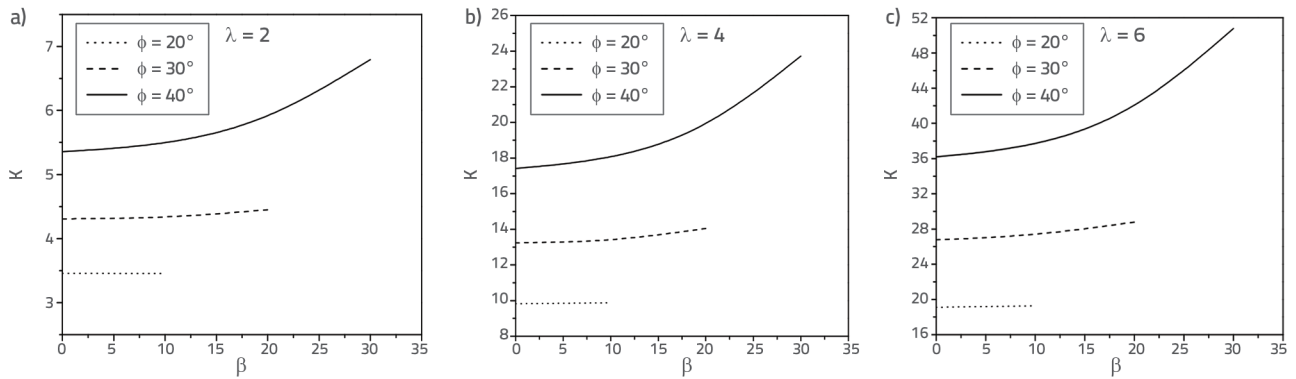
Figure 7. Variation of pullout factor (K) with oblique pullout angle ($\beta°$) for different friction angle (ϕ) za) $\lambda = 2$; b) $\lambda = 4$; c) $\lambda = 6$

the angle of obliquity along with the soil parameters. The rate of increase in the inclined pullout factor was found to be more significant for denser sand, owing to an increase in the failure zone. Furthermore, the obliquity of the tie rod might be beneficial, resulting in improved pullout. However, this observation remains valid up to a certain angle of obliquity, that is, the critical angle of inclination of the pullout, beyond which the uplift capacity is reduced [30]. This may be attributed to the corresponding alteration in the angle of inclination of the rupture surface towards the right and left. Nevertheless, this study is limited to $\beta \leq \phi$, due to which the critical obliquity angle is not reported.

4.2.3. Effect of embedment ratio (λ)

The embedment ratio (λ) plays a significant role in determining the pullout capacity of an anchor. As the embedment ratio increases, the failure zone around the anchor also expands, resulting in a higher pullout capacity for the strip anchor. An increase in the pullout factor due to an increase in embedment ratio can be observed in both the vertical and oblique pullout scenarios.
In Figure 6.a, the pullout factor for $\beta = 0°$ increases by 4.5 times when the embedment ratio rises from 2 to 6, at a soil friction angle (ϕ) of 30°. Similarly, in Figure 6.b, the oblique pullout factor increases by 5.27 and 5.47 times, for $\beta = 10°$ and 20° respectively, for the same increase in embedment ratio. These observations confirm that an increase in the embedment ratio results in higher pullout due to the enlarged size of the failure zone.

4.2.4. Effect of orientation of tie rod (β)

Figure 7 illustrates that as the orientation of the tie rod (β) increases, the pullout factor also increases. This increase is likely due to the fact that as the orientation of the tie rod increases, the failure zone on the inclined side of the tie rod also expands, resulting in greater pullout capacity. However, it is important to note that the inclination of the tie rod is limited by the soil friction angle, which is a property of the soil representing the maximum angle at which the soil can resist sliding.

4.3. Layered cohesionless soil

An analysis was performed to estimate the pullout capacity of a horizontal strip anchor embedded in two layers. The results of the analysis are presented in terms of the optimum pullout factor (K) and the optimum failure angles of the soil (α_{RT}, α_{RB}, α_{LT}, and α_{LB}). The factor (K) was calculated for different combinations of soil layers:
Case a: Loose sand layer ($\phi_T = 30°$) overlying a dense sand layer ($\phi_B = 40°$) with $\gamma_T \leq \gamma_B$.
Case b: Dense sand layer ($\phi_T = 40°$) overlying a loose sand layer ($\phi_B = 30°$) with $\gamma_T \geq \gamma_B$.

It is considered that the friction angle of the sand layer primarily depends on the relative density because denser packing of particles leads to higher relative density [33, 34]. The interlocking behavior of sand particles under load causes them to resist further movement more effectively, thereby increasing the frictional angle.

4.3.1. Pullout capacity of anchor in the layered sand ($\beta = 0°$)

It must be noted that the pullout force is sensitive to the thickness of the dense stratum. Hence, the thickness of the dense sand layer (H_{Dense}/H) was considered an additional parameter in this analysis. The results are presented in Figures 8(a) and 8(b) for Cases (a) and (b), respectively. As expected, it can be observed from Figure 8.a that the pullout factor (K) increases with the increase in the thickness of the bottom dense sand layer. For H_{Dense}/H values of 0 and 1, which represent the extreme cases of no dense sand layer and no loose sand layer, respectively, the magnitudes of the pullout factor correspond to those of homogeneous ground with friction angles of 30° and 40°, respectively, for Case (a) and vice versa for Case (b).
The magnitude of the pullout factor (K) was found to increase with the increasing thickness of the dense sand layer and embedment ratio, irrespective of cases (a) and (b). These results suggest that the relative positions of the two layers significantly affect the pullout capacity of strip anchors. When the loose sand layer was placed over the dense sand layer, the pullout factor
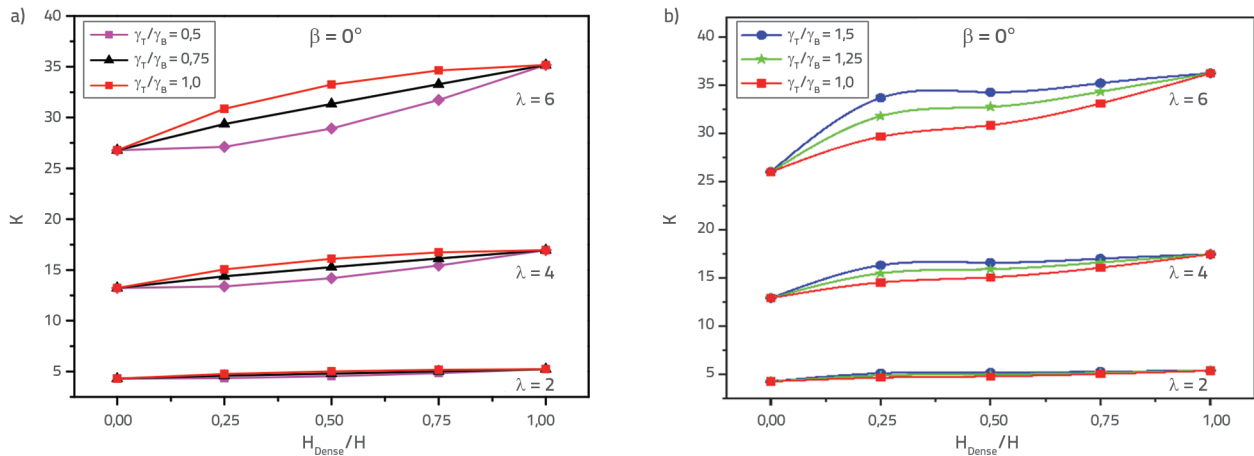
Figure 8. Variation of vertical pull-out factor (K) with H_{Dense}/H for: a) Case (a) $\gamma_T \leq \gamma_B$; b) Case (b) $\gamma_T \geq \gamma_B$
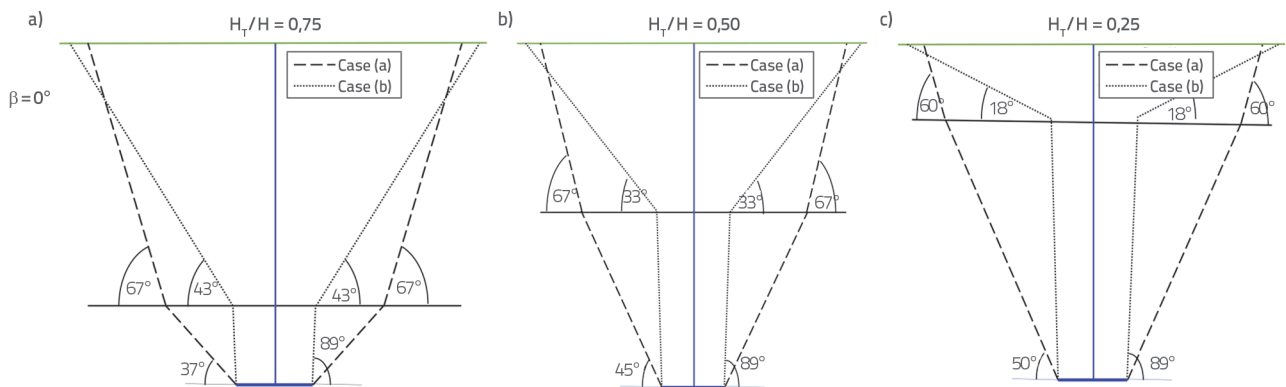
Figure 9. Geometrical representation of failure angle for embedment ratio (λ = 2, 4 i 6) with ϕ_T = 30° and ϕ_B = 40° za: a) H_T/H = 0,75; b) H_T/H = 0; c) H_T/H = 0,25

(K) increased significantly. This increase may be due to the fact that the dense sand layer provides a stable base for the anchor, while the loose sand layer offers a larger failure surface, leading to a notable increase in pullout capacity.

Furthermore, the difference in the magnitude of K between these two cases became more significant as the ratio of the thickness of the dense sand layer to the total thickness (H_{Dense}/H) increased, particularly when the heights of the top (H_T) and bottom (H_B) layers were nearly equal. This indicates that the thicknesses and relative positions of the two layers should be carefully considered when placing the anchor system. This can be understood by investigating the failure surfaces generated by the anchor during pullout, as shown in Figure 9.

Figure 9 illustrates the comparative failure surfaces for the maximum pullout factor in cases (a) and (b). In case (a), where a loose-to-dense ratio was observed, as the H_T/H (height of the top layer divided by the total embedment depth) increased, the failure angle decreased for the bottom layer but increased for the top layer.

The failure surfaces are symmetric since the pullout is vertical (β = 0°). Figure 9 illustrates a typical failure pattern for Case (b), indicating the development of a funnel-shaped depression

on the surface. This demonstrates that the bottom loose sand layer became unstable and slid into the depression, resulting in the cascading failure of the top layer in Case (b). However, the soil contribution to the resistance of the pullout forces was greater in Case (a), resulting in a stable failure zone.

4.3.2 Oblique pullout of anchor in the layered sand ($\beta \neq 0°$)

Figure 10 displays the curves for the pullout factor (K) and embedment ratio in the two-layered sand for case (a) obtained through limit equilibrium analysis. It shows the relationship between the maximum pullout and the ratio of the thickness of the bottom dense layer to the total embedment depth (H_{Dense}/H), considering oblique pullout angles of 10° and 20°. Similar to the observation of vertical pullout behavior, the value of K increased as the ratio H_{Dense}/H (dense bed thickness to total embedment depth) increased, indicating an increasing pullout factor as the depth of the dense bed increased.

Figure 11 shows curves depicting the pullout factor in relation to the ratio of the dense-bed thickness to the total embedment depth (H_{Dense}/H) for Case (b). The pullout factor increases with the H_{Dense}/H. Additionally, the pullout factor increases with an
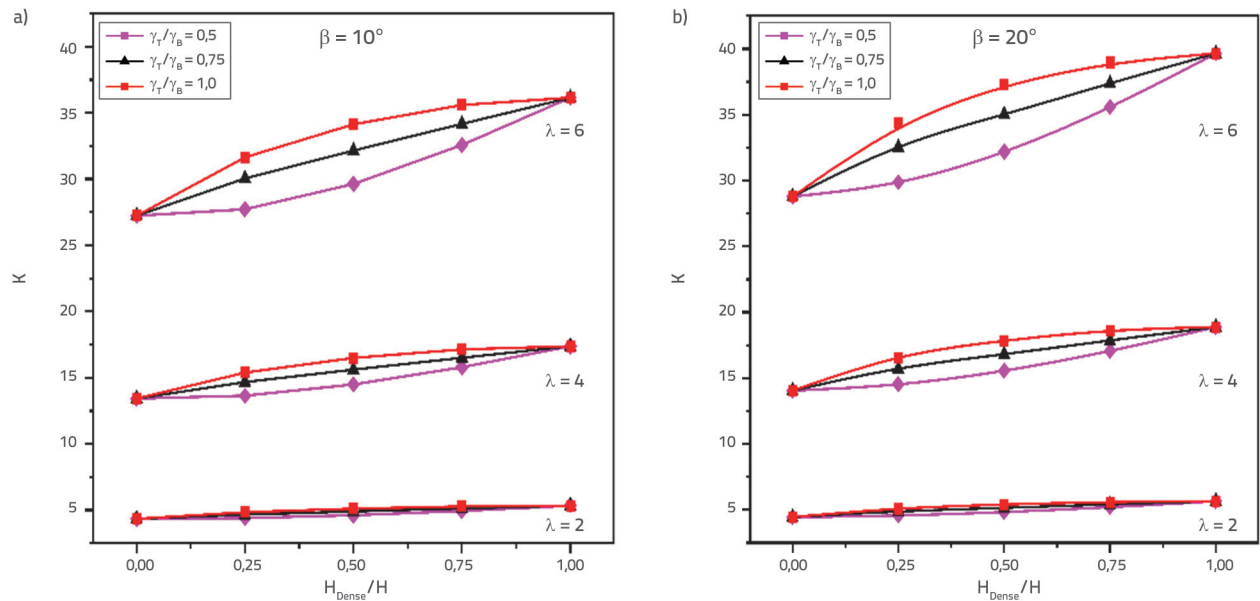
Figure 10. Variation of oblique pull-out factor (K) with H_{Dense}/H for Case (a) $\gamma_T \geq \gamma_B$; a) $\beta = 10°$; b) $\beta = 20°$
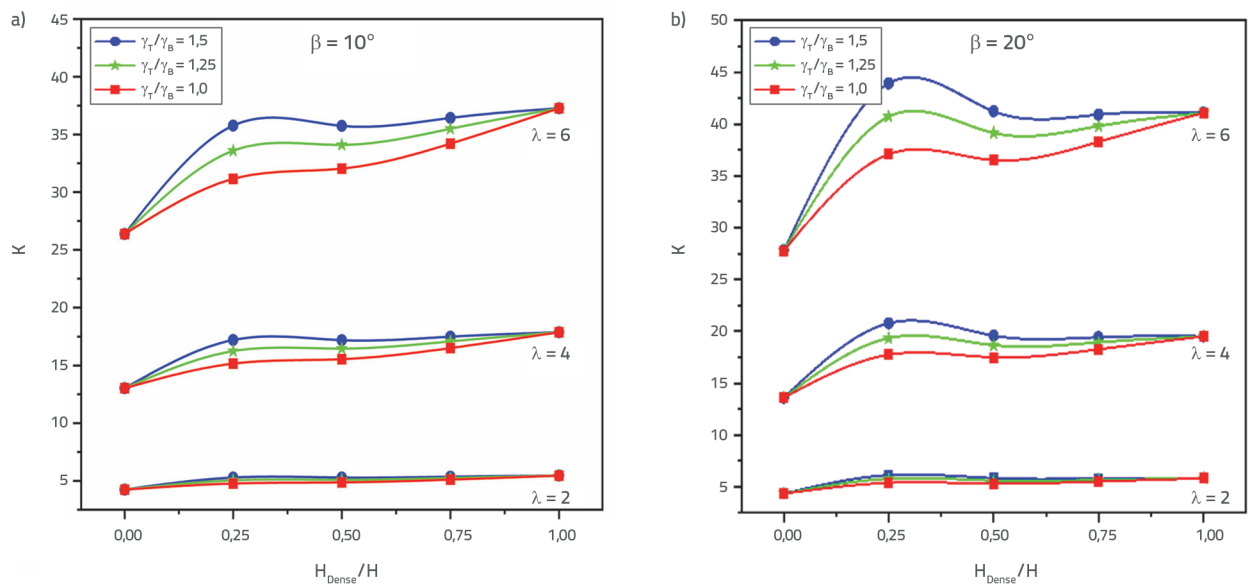
Figure 11. Variation of oblique pullout factor (K) with H_{Dense}/H for Case (b) $\gamma_T \geq \gamma_B$; a) $\beta = 10°$; b) $\beta = 20°$

increase in obliquity, i.e., the orientation of the tie rod. Therefore, inclined pullout has a positive effect on the anchor, leading to an increase in its pullout capacity.

Figure 12 illustrates the geometrical failure angles for various embedment ratios, considering Cases (a) and (b). Unlike previous assumptions made by other researchers, the failure angle in this study was determined at the corresponding maximum

pullout factor. Similar to Figure 8, the comparison focused on the failure angle of the top layer in relation to the total depth of embedment (H_T/H). It can be observed that as the failure angle increases, it approaches the angle of obliquity. Case (b) also exhibited a funnel-shaped failure pattern during the oblique pullout. However, the failure of the soil occurred in a wedge form in Case (a), as considered during the analysis.
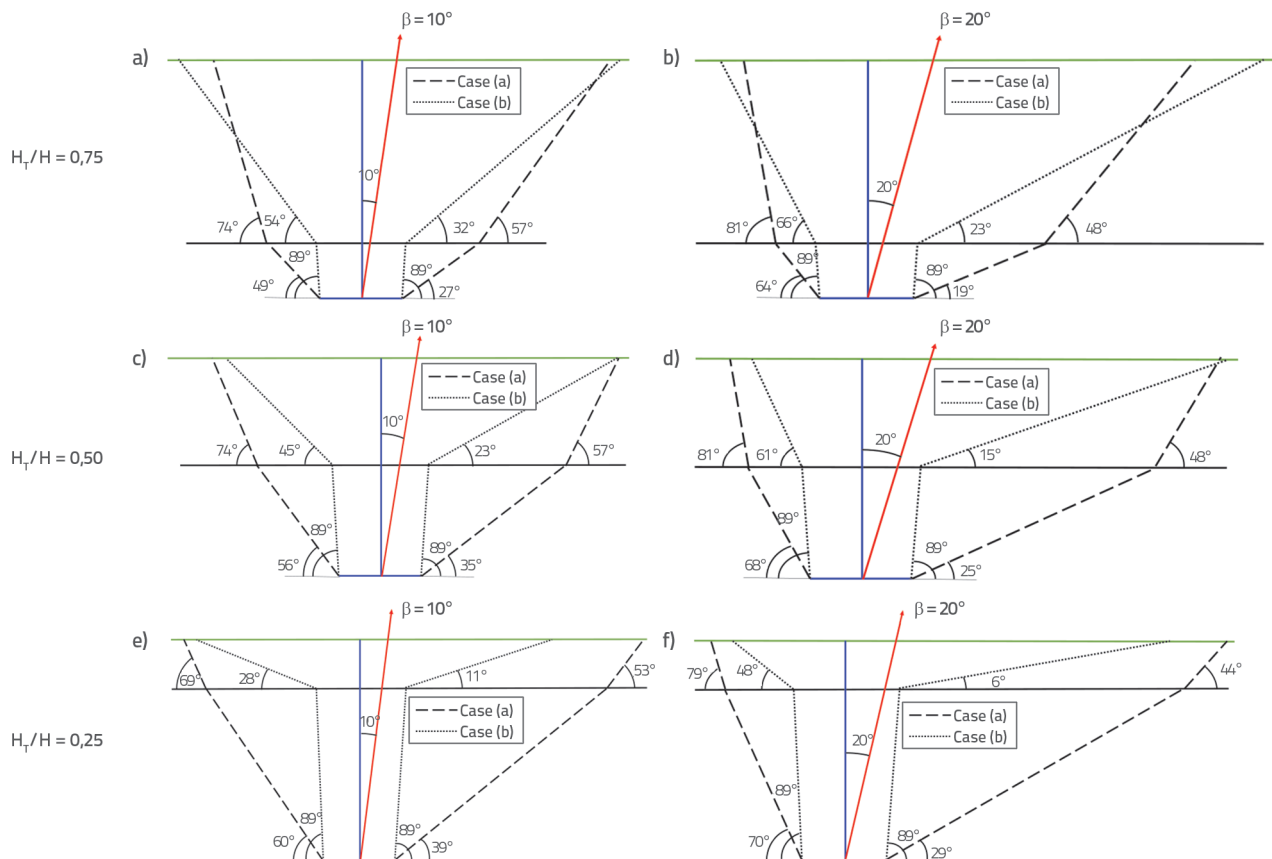
Figure 12. Geometrical representation of failure angle for embedment ratio (λ = 2, 4, & 6): a) H_t/H = 0,75 and β = 10°; b) H_t/H = 0,5 and β = 10°; c) H_t/H = 0,25 and β = 10°; d) H_t/H = 0,75 and β = 20°; e) H_t/H = 0,5 and β = 20°; f) H_t/H = 0,25 and β = 20°

5. Conclusion

The present analysis utilized the limit equilibrium method in association with the Kötter equation to determine the pullout factor and trace the failure surface of obliquely loaded horizontal strip anchors in both homogeneous and layered sandy strata. This study showed that the pullout factor increases with the inclination of the pullout in both homogeneous and two-layered medium-dense sand. The predicted values also correspond to the failure angle of the planar surface, which varies with the pullout inclination. Comparison and validation studies were conducted to demonstrate the accuracy and reliability of the proposed approach for predicting the pullout capacities of obliquely loaded horizontal strip anchors.

REFERENCES

[1] Meyerhof, G.G, Adams, J.I.: The Ultimate Uplift Capacity of Foundations, Canadian Geotechnical Journal, 5 (1968) 4, pp. 225–244.

[2] Rao, K.S.S., Kumar, J.: Vertical Uplift Capacity of Horizontal Anchors, Journal of Geotechnical Engineering, 120 (1994) 7, pp. 1134–1147. https://doi.org/10.1061/(ASCE)0733-9410(1994)120:7(1134)

[3] Deshmukh, V.B., Dewaikar, D.M, Choudhury, D.: Analysis of Rectangular and Square Anchors in Cohesionless soil, International Journal of Geotechnical Engineering, 4 (2010) 1, pp. 79–87. https://doi.org/10.3328/IJGE.2010.04.01.79-87

[4] Deshmukh, V.B., Dewaikar, D.M., Choudhury, D.: Computations of Uplift Capacity of Pile Anchors in Cohesionless Soil, Acta Geotechnica, 5 (2010) 2, pp. 87–94. https://doi.org/10.1007/s11440-010-0111-6

[5] Deshmukh, V B., Dewaikar, D.M., Choudhary, D.: Uplift Capacity of Horizontal Strip Anchors in Cohesionless Soil, Geotechnical and Geological Engineering, 29 (2011) 6, pp. 977–988. https://doi.org/10.1007/s10706-011-9430-0

[6] Dewaikar, D.M., Deshmukh, V.B.: Estimation of Uplift Capacity of Horizontal Plate Anchor in Sand, Global Journal of Researches in Engineering, 19 (2019) 4, pp. 19–37. https://doi.org/10.34257/gjreevol19is4pg19

[7]   Mors, H.: The behavior of mast foundations subjected to tensile forces, Bautechnik, 36 (1959) 10, 367–378.

[8]   Downs, D.I., Chieurzzi, R.: Transmission tower foundations. J. Power, Div. ASCE, 88 (2) 1966, pp. 91–114.

[9]   Matsuo, M.: Study on the uplift resistance of footing (I), Japanese Soc. Soil Mechanics & Foundation Engineering, Soils and Foundations, 7 (1967) 4, pp. 1-37.

[10] Veesaert, C.J., Clemence, S.P.: Dynamic pullout resistance of anchors, Proc. Int. Symp. Soil-Structure Interaction, Rourkee, India, 1 (1977), pp. 389–397.

[11] Kumar, J., Kouzer, K.M.: Vertical Uplift Capacity of Horizontal Anchors using Upper Bound Limit Analysis and Finite Elements, Canadian Geotechnical Journal, 45 (2008) 5, pp. 698–704, https://doi.org/10.1139/T08-005

[12] Das, B.M., Seeley, G.R.: Inclined load resistance of anchors in sand, Proceedings of the American Society of Civil Engineers 2 (1975) (GT9), 995–1003.

[13] Murray, E.J., Geddes, J.D.: Uplift of Anchor Plates in Sand, Journal of Geotechnical Engineering, 113 (1987) 3, pp. 202-215.

[14] Liu, J., Liu, M., Zhu, Z.: Sand Deformation Around an Uplift Plate Anchor, Journal of Geotechnical and Geoenvironmental Engineering, 138 (2012) 6, pp. 728–737, https://doi.org/10.1061/(asce)gt.1943-5606.0000633

[15] Chow, S.H., Le, J., Forsyth, M., O'Loughlin, C.: Capacity of Vertical and Horizontal Plate Anchors in Sand Under Normal and Shear Loading, Proc. of the 9th International Conference of Physical Modelling in Geotechnics (ICPMG2018), pp. 559–564, 2018 https://doi.org/10.1201/9780429438660-82

[16] Zhuang, P., Yue, H., Song, X., Sun, R., Wu, J., Guan, Y.: Ultimate Pullout Capacity of Single Vertical Plate Anchors in Sand, Marine Georesources and Geotechnology, (2021), pp. 1–19, https://doi.org/10.1080/1064119X.2021.1950247.

[17] Ilamparuthi, K., Dickin, E.A., Muthukrisnaiah, K.: Experimental investigation of the uplift behaviour of circular plate anchors embedded in sand, Canadian Geotechnical Journal, 39 (2002) 3, 648–664, https://doi.org/10.1139/t02-005.

[18] Dickin, B.E.A.: Uplift Behaviour of Horizontal Anchor, Journal of Geotechnical Engineering, 114 (1988) 11, pp. 1300–1317

[19] Khatri, V.N., Kumar, J.: Effect of Anchor Width on Pullout Capacity of Strip Anchors in Sand, Canadian Geotechnical Journal, 48 (2011) 3, pp. 511–517, https://doi.org/10.1139/T10-082

[20] Bhattacharya, P., Kumar, J.: Uplift Capacity of Anchors in Layered Sand Using Finite-Element Limit Analysis: Formulation and Results, International Journal of Geomechanics, 16 (2016) 3, pp. 04015078-1-15, https://doi.org/10.1061/(asce)gm.1943-5622.0000560

[21] Kumar, J.: Uplift Resistance of Strip and Circular Anchors in a Two Layered Sand, Soils and Foundations, 43 (2003) 1, pp. 101–107, https://doi.org/10.3208/sandf.43.101

[22] Ghosh, P.: Seismic Vertical Uplift Capacity of Horizontal Strip Anchors using Pseudo-Dynamic Approach, Computers and Geotechnics, 36 (2009) 1–2, pp. 342–351, https://doi.org/10.1016/j.compgeo.2008.01.002

[23] Sahoo, J.P., Kumar, J.: Vertical Uplift Resistance of Two Horizontal Strip Anchors with Common Vertical Axis, International Journal of Geotechnical Engineering, 6 (2012) 4, pp. 485–495, https://doi.org/10.3328/IJGE.2012.06.04.485-495.

[24] Bhattacharya, P., Kumar, J.: Vertical Pullout Capacity of Horizontal Anchor Plates in the Presence of Seismic and Seepage Forces, Geomechanics and Geoengineering, 9 (2014) 4, pp. 294–302, https://doi.org/10.1080/17486025.2014.902116

[25] Sahoo, J.P., Ganesh, R.: Vertical Uplift Resistance of Rectangular Plate Anchors in Two Layered Sand, Ocean Engineering, 150 (2018), pp. 167–175, https://doi.org/10.1016/j.oceaneng.2017.12.056

[26] Kumar, J., Rahaman, O.: Vertical Uplift Resistance of Horizontal Plate Anchors for Eccentric and Inclined Loads', Canadian Geotechnical Journal, 56 (2019) 2, pp. 290–299, https://doi.org/10.1139/cgj-2017-0515.

[27] Kötter, F.: Die Bestimmung des Drucks an gekrümmten Gleitflächen, eine Aufgabe aus der Lehre vom Erddruck, Sitzungsberichte der Akademie der Wissenschaften, Berlin, pp. 229–233, 1903, urn:nbn:de:hebis:30-1124329

[28] Rangari, S.M., Choudhury, D., Dewaikar, D.M.: Pseudo-Static Uplift Capacity of Horizontal Strip Anchors, Geo-Frontiers, (2011), pp. 1821–1831, https://doi.org/10.1061/41165(397)186

[29] Rangari, S.M., Choudhury, D., Dewaikar, D.M.: Pseudo-Static Uplift Capacity of Obliquely Loaded Horizontal Strip Anchor in Cohesionless Soil, GeoCongress © ASCE 2012, pp. 185–194, https://doi.org/10.1061/9780784412121.02

[30] Rangari, S.M., Choudhury, D., Dewaikar, D.M.: Computations of Seismic Passive Resistance and Uplift Capacity of Horizontal Strip Anchors in Sand, Geotechnical and Geological Engineering, 31 (2013) 2, pp. 569–580, https://doi.org/10.1007/s10706-012-9609-z

[31] Rangari, S.M., Choudhury, D., Dewaikar, D.M.: Estimation of Seismic Uplift Capacity of Horizontal Strip Anchors using Pseudo-Dynamic Approach, KSCE Journal of Civil Engineering, 17 (2013) 5, pp. 989–1000, https://doi.org/10.1007/s12205-013-0046-1

[32] Rangari, S.M., Choudhury, D., Dewaikar, D.M.: Seismic uplift capacity of shallow horizontal strip anchor under oblique load using pseudo-dynamic approach", Soils and Foundations, 53 (2013) 5, pp. 692–707, https://doi.org/10.1016/j-sandf.2013.08.007

[33] Ching, J., Guan-Hong Lin, Jie-ru Chen, and Kok-Kwang Phoon: Transformation models for effective friction angle and relative density calibrated based on generic database of coarse-grained soils, Canadian Geotechnical Journal, 54 (2017) 4, pp. 481-501, https://doi.org/10.1139/cgj-2016-0318

[34] Mujtaba, H., Farooq, K., Sivakugan, N, Das, B.M.: Evaluation of Relative Density and Friction Angle Based on SPT-N Values, KSCE Journal of Civil Engineering, 22 (2018) 2, pp. 572-581, https://doi.org/10.1007/s12205-017-1899-5